

5. P. T. Marshall, *J. Cons. Int. Explor. Mer.* **23**, 173 (1957).
6. H. U. Sverdrup, *ibid.* **18**, 287 (1953).
7. A. J. Clarke, *Deep-Sea Res.* **25**, 41 (1979); L. P. Røed and J. J. O'Brien, *J. Geophys. Res.* **88**, 2863 (1983).
8. J. R. Buckley, T. Gammelsrod, J. A. Johannessen, O. M. Johannessen, L. P. Røed, *Science* **203**, 165 (1979); O. M. Johannessen, J. A. Johannessen, J. Morison, B. A. Farrelly, E. A. S. Svendsen, *J. Geophys. Res.* **88**, 2755 (1983).
9. For example, surface nitrate concentrations in waters south of the Antarctic convergence rarely fall below 10 μM [S. Z. El-Sayed, in *Antarctic Ecology*, M. W. Holdgate, Ed. (Academic Press, New York, 1970)]. In our study the mean surface nitrate concentration was 10.2 μM (D. Nelson *et al.*, in preparation).
10. S. L. Smith, W. O. Smith, L. A. Codispoti, paper presented at the American Geophysical Union/American Society of Limnology and Oceanography Ocean Science Meeting, New Orleans, February 1984.
11. A. C. Palmisano and C. W. Sullivan, *Polar Biol.* **2**, 171 (1983); S. F. Ackley, K. R. Buck, S. Taguchi, *Deep-Sea Res.* **26A**, 269 (1979); R. A. Horner, *Oceanogr. Mar. Biol.* **14**, 167 (1976).
12. L. Schandelmeyer and V. Alexander, *Limnol. Oceanogr.* **26**, 935 (1981); T. J. Hart, *Discovery Rep.* **21**, 263 (1942).
13. Three sections were sampled, with stations 36 through 43 being the middle transect. The same section was surveyed 5 days earlier [W. O. Smith and D. M. Nelson, in *Fourth Symposium on Antarctic Biology*, L. W. Siegfried, Ed. (Elsevier, Amsterdam, in press)].
14. A CTD is an instrument that continuously records conductivity, temperature, and pressure as it is lowered through the water. From these measurements salinity and density can be calculated.
15. Chlorophyll was analyzed fluorometrically on samples filtered through Gelman A/E glass fiber filters and extracted in 90 percent acetone. Particulate carbon was collected by filtration of seawater through precombusted Gelman A/E glass fiber filters, dried at 60°C, and analyzed on a Perkin-Elmer model 240B elemental analyzer. Biogenic silica, a measure of the silicon incorporated into diatom and silicoflagellate tests, was determined by filtering seawater through 0.4- μm Nuclepore filters, drying the filters at 60°C, digesting the filters in hot sodium hydroxide, and determining the resulting concentration of silicic acid by colorimetry.
16. D. L. Wilson, W. O. Smith, D. M. Nelson, paper presented at the American Geophysical Union/American Society of Limnology and Oceanography Ocean Science Meeting, New Orleans, February 1984.
17. R. S. Truesdale and T. B. Kellogg, *Mar. Micropaleon.* **4**, 13 (1979).
18. L. A. Hobson, D. W. Menzel, R. T. Barber, *Mar. Biol.* **19**, 298 (1973).
19. W. M. Krebs, *Micropaleontology* **29**, 267 (1983).
20. T. R. Parsons, M. Takahashi, B. Hargrave, *Biological Oceanographic Processes* (Pergamon, New York, 1977), pp. 50–60.
21. W. K. W. Li, in *Primary Productivity in the Sea*, P. Falkowski, Ed. (Plenum, New York, 1980), pp. 259–279.
22. D. M. Nelson and L. I. Gordon, *Geochim. Cosmochim. Acta* **46**, 491 (1982).
23. S. leJehan and P. Treuger, in *Fourth Symposium on Antarctic Biology*, L. W. Siegfried, Ed. (Elsevier, Amsterdam, in press).
24. O. Holm-Hansen *et al.*, in *Adaptations within Antarctic Ecosystems*, G. Llano, Ed. (Gulf, Houston, 1977), pp. 11–50.
25. J. C. Jennings, L. I. Gordon, D. M. Nelson, *Nature (London)* **308**, 51 (1984).
26. G. E. R. Deacon, *Deep-Sea Res.* **29**, 1 (1982); J. Tranter, *Oceanogr. Mar. Biol.* **20**, 11 (1982).
27. I. Everson, *The Living Resources of the Southern Ocean* (Food and Agricultural Organization, Rome, 1977), pp. 27–33.
28. D. DeMaster, *Geochim. Cosmochim. Acta* **45**, 1715 (1981); S. E. Calvert, in *Silicon Geochemistry and Biogeochemistry*, S. R. Aston, Ed. (Academic Press, New York, 1983), pp. 143–186; D. DeMaster and P. Hoffman, in preparation.
29. Supported by NSF grant DPP81-19572 and by the Office of Naval Research while one of us (W.O.S.) occupied the Arctic Chair in Marine Science at the Naval Postgraduate School, Monterey, Calif. J. Ahern, M. Carbonell, J. Elser, S. Moore, C. Weimer, P. Whaling, and D. Wilson assisted in the study. Order of authorship was determined by coin toss.

13 June 1984; accepted 11 October 1984

Sea-Floor Hydrothermal Activity Links Climate to Tectonics: The Eocene Carbon Dioxide Greenhouse

Abstract. *Two important findings of recent ocean-floor drilling in the southeast Pacific (Deep Sea Drilling Project Leg 92) are (i) that sea-floor hydrothermal activity may fluctuate through time by as much as an order of magnitude and (ii) that episodes of greatest hydrothermal flux correspond to times when ridge-transform plate boundaries are undergoing major changes in their configuration rather than to known times of increased spreading rate or volcanism. Evidence is presented here in support of the hypothesis that heightened hydrothermal activity induced by the Eocene tectonic activity caused a global greenhouse effect, which may represent the long-sought-after historical analog to the carbon dioxide-induced global warming expected to occur by the middle of the next century.*

The idea that changes in atmospheric CO₂ concentrations can affect global surface temperatures was first postulated nearly a century ago (1–3). This connection not only is now well documented and widely accepted but also has aroused much concern. Increased CO₂ inputs during the next several decades, primarily from the cumulative effects of deforestation and fossil-fuel combustion, are expected to double the atmospheric CO₂ load thought to have been present in 1900 (4). Various numerical models predict that this CO₂ doubling will lead to a greenhouse effect, manifested as an in-

crease of about 1.5° to 4.5°C in the mean global surface temperature by the middle of the next century (5).

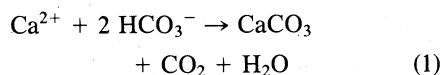
This anthropogenically induced change in atmospheric composition has been viewed as both a massive and an unprecedented geophysical experiment (5, 6). That it is occurring now on a large scale is clear; it is far less certain, however, that it has not occurred before. Indeed, there is abundant paleontological, paleoceanographic, and paleogeographic evidence in support of the idea that relatively warmer periods occurred during the past (7–9). Revelle (3) has suggested that

paleoclimatic reconstructions of these periods could be used to evaluate and verify the predictions of mathematical models (which contain certain troublesome uncertainties) and could provide useful clues to the consequences of future warming trends. Unfortunately, the application of this earth-model approach to past time periods is hampered by a limited data base and inherent chronological errors, whereas investigations of more recent periods must grapple with uncertainties concerning the role of CO₂ in global warming events. For example, both the warm climate of the early Holocene and glacial-interglacial temperature oscillations have been related to changes in the earth's orbit. These changes in atmospheric CO₂ concentrations may have been responses to rather than causes of the associated climate changes (5). For this reason, one conclusion of a recent review of studies concerning the anticipated CO₂ greenhouse effect was that there is no satisfactory historical analog (5). We suggest here that CO₂-induced climate changes have occurred, that they were caused by pulsations in the intensity of sea-floor hydrothermal activity induced by tectonic rearrangements of sea-floor spreading centers, and that the most obvious example of this process occurred in the early Eocene.

This suggestion of an inferred link between ocean tectonics and atmospheric CO₂ concentrations is based upon correlations between certain parameters of tectonism (for example, spreading rates) and sea level changes, the occurrence of oolites in the stratigraphic record of the Phanerozoic, and computer-simulated variations in the carbonate-silicate geochemical cycle over the past 100 million years (m.y.) (10–13). A direct chemical link between sea-floor processes and CO₂ fluxes was revealed recently by the discovery of widespread hydrothermal activity along oceanic ridges. Fissures and fractures formed in fresh ridge-crest basalt as it cools and is rifted apart provide conduits for the circulation of cold bottom waters into the underlying crust. The circulating seawater penetrates to depths of a few kilometers, reacts chemically with hot basalt at temperatures in excess of 300°C, and emerges as hot springs along the ocean floor (14). The chemical exchanges that occur during this process include the removal of magnesium and sulfate from seawater and concomitant enrichment of calcium, potassium, silica, iron, manganese, and other trace elements within the hydrothermal solution (14–18).

The chemical exchange of calcium for magnesium in this process is particularly

relevant to the CO₂ cycle. Both laboratory and field investigations have shown that for each Mg²⁺ that is removed from seawater there occurs a replacement by an essentially stoichiometrically equivalent amount of Ca²⁺ (12, 19, 20). The only significant process that balances Ca²⁺ inputs to the oceans is the precipitation of (biogenic) CaCO₃, which is accompanied by the formation of CO₂:



Estimates of the total annual hydrothermal Ca²⁺ input into the oceans can be used to assess the relative contribution of hydrothermal activity to the modern global CO₂ budget. The total fluvial input of HCO₃⁻ to the oceans is about 3.20×10^{13} mol year⁻¹; however, if we exclude hydrothermal activity, only about 66 percent of this input can be accounted for by all other known removal processes (21, 22). Assuming that the "excess" HCO₃⁻ (1.09×10^{13} mol year⁻¹) is exactly balanced by hydrothermal Ca²⁺ inputs according to Eq. 1, we calculate the hydrothermal Ca²⁺ input to be 5.45×10^{12} mol year⁻¹. This value is in good agreement with other independent estimates of the hydrothermal Ca²⁺ flux: 5.2×10^{12} mol year⁻¹, based on the carbonate-silicate geochemical cycle of present-day oceans (12) and 4.3×10^{12} mol year⁻¹, based on an extrapolation of Ca²⁺ concentrations in hydrothermal plumes at the Galápagos spreading ridge (17). If we take the hydrothermal Ca²⁺ input to be 5×10^{12} mol year⁻¹ and the fluvial Ca²⁺ input to be 12.5×10^{12} mol year⁻¹ (22), then the total Ca²⁺ input to the oceans is about 17.5×10^{12} mol year⁻¹. Assuming steady-state conditions and recognizing that for each mole of Ca²⁺ input 1 mol of CO₂ is produced, we estimate that sea-floor hydrothermal activity accounts for about 29 percent of the total ocean contribution to atmospheric CO₂. According to recent budget calculations, the oceans contribute between 47 percent (3) and 75 percent (12) of the total global atmospheric CO₂ input, depending primarily upon whether short-term biological cycles or long-term geochemical cycles are emphasized. In any case, our calculations indicate that sea-floor hydrothermal activity is a significant factor in the present-day CO₂ budget, accounting for about 14 to 22 percent of the total atmospheric CO₂ input.

If during certain times in the geologic past the intensity of hydrothermal activity was significantly greater than today, then it is reasonable to argue that these periods represent analogs to CO₂-in-

duced climatic changes. Leg 92 of the Deep Sea Drilling Project (DSDP), which crossed the East Pacific Rise (EPR) at 19°S, was undertaken to provide the first direct documentation of the geologic history of ridge-axis hydrothermal activity. Following "conventional wisdom," we had expected that the hydrothermal record recovered would reflect the history in the Pacific region of mid-plate and plate-margin volcanism and of spreading-rate fluctuation (23–25). It did not. Hydrothermal activity in the southeast Pacific reaches relative maxima of five to ten times present values, based on mass-accumulation rates of iron-rich sediment, in the earliest Miocene and the late Miocene (26–28). Pitman's (25) compilation of global spreading rates along 12 spreading centers shows that five display constant spreading throughout the Cenozoic, three show marked rate reductions during the Paleogene and are constant since then, and four fluctuate by 20 to 40 percent (two increase and two decrease in rate). Episodes of hydrothermal activity documented by the Leg 92 Scientific Party (27, 28) therefore do not appear to correspond to spreading-rate fluctuations. On the other hand, these episodes do coincide with the two periods of ridge-jumping and reorganization of divergent and transform plate boundaries along the EPR that occurred approximately 20 to 25 m.y. ago (29) and 6 to 8 m.y. ago (30).

Other information appears to confirm that hydrothermal input to the oceans depends on factors other than spreading rate, primarily tectonism. For example, the accumulation of metalliferous sediments at DSDP site 319, which lies east of the EPR in the Bauer Deep, displays an approximately fivefold increase in hydrothermally derived elements about 8 m.y. ago (31). At this time the spreading axis jumped 800 km west from the fossil Galápagos Rise, now in the middle of the Nazca Plate, to the present EPR (30). During June and July 1984, the Canadian research submarine *Pisces-4*, diving on the Explorer Ridge southwest of British Columbia, encountered ophiolite-scale sulfide deposits along the spreading axis. Scientists on that expedition estimated that the slow-spreading Explorer Ridge is producing one to two orders of magnitude more hydrothermal material than (an equivalent length of) the fast-spreading EPR (32).

The early to middle Eocene was also a time of greatly enhanced accumulation of hydrothermally derived material, especially iron, in Pacific sediments (26, 33). The bulk hydrothermal and hydrogeous components of pelagic clay sec-

tions at DSDP site 464 (34) and core LL44-GPC3 (35) show their maximum Cenozoic accumulation 50 to 55 m.y. ago. These clear indications of enhanced hydrothermal activity are important because the early Eocene is the time of the last global-scale episode of ridge-jumping and general reorganization of sea-floor spreading centers and has long been recognized as having the warmest and most humid Cenozoic climate.

We suggest that these two events, increased tectonism and warm climate, are cause and effect linked by the process described above. Recalculation of the carbonate mass balance model of Berner *et al.* (12) with a fourfold increase of hydrothermal calcium input to the oceans yields a doubling of CO₂ in the oceans and thus a doubling of CO₂ in the atmosphere, assuming the two concentrations are linearly related.

If our hypothesis is correct, one would expect to find evidence in the geologic record for the following events approximately 50 m.y. ago: (i) a global warming above preexisting temperatures of a magnitude similar to or greater than that predicted for the modern case; (ii) possible increased humidity; (iii) a decreased pole-to-equator temperature gradient; (iv) increased accumulation of hydrothermal iron in deep-sea sediments; (v) increased accumulation of silicon in deep-sea sediments; and (vi) increased Ca²⁺ concentrations in seawater and increased CaCO₃ accumulation in marine sediments. There is strong evidence for all six of these apparently related phenomena.

The Eocene global warming has long been recognized from both terrestrial (7, 36–38) and oceanic (8, 39, 40) records. Oxygen isotope data from oceanic foraminifera provide some quantification of this warming, which is about 5°C above Paleocene values (41). Humid Eocene climates are suggested by the prevailing flora (36–38) and the very low amounts of eolian dust that were transported to the oceans (42, 43). The early to middle Eocene is also the time of the warmest high-latitude regions (9) and thus the lowest pole-to-equator temperature gradients, perhaps less than half that of the present (40, 41). Recent work on the Cenozoic record of eolian dust accumulation suggests that a rather sudden large reduction in the intensity of atmospheric circulation occurred in the early to middle Eocene, which would suggest a rapid decrease in the temperature gradient (42, 43).

The input of both hydrothermal (26, 35) and opaline (44, 45) materials to the sea floor increased severalfold 50 m.y.

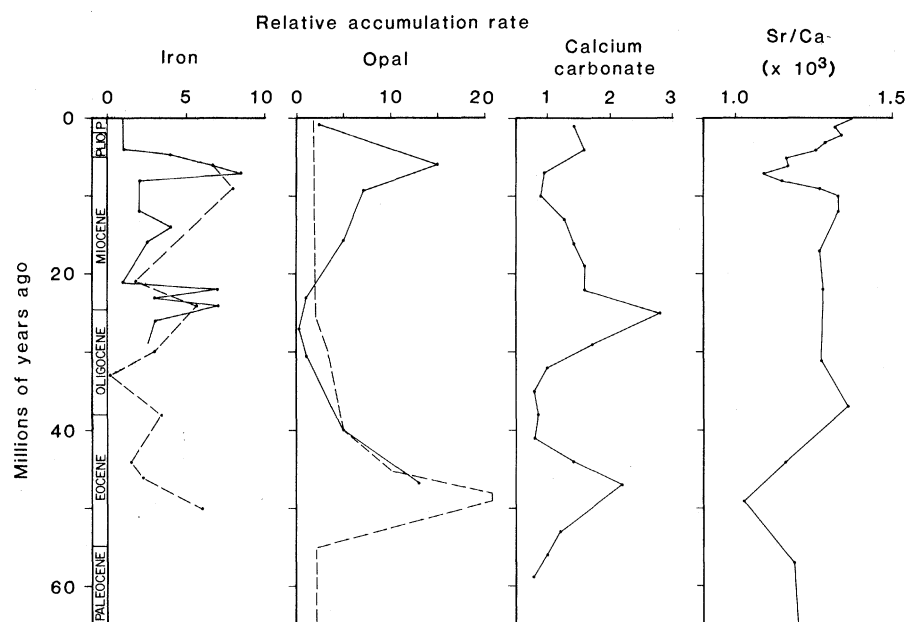


Fig. 1. Relative accumulation rates of iron (26–28), opal (44, 45), and CaCO_3 (51) and the Sr/Ca ratio (49) in forams. Increases in all three accumulation rates and a decrease in the Sr/Ca ratio occurred in the early to middle Eocene, about 50 m.y. ago.

ago (Fig. 1). Most of the Eocene opal has undergone diagenetic conversion to the widespread chert deposits of that age, and so accurate opaline flux values for that time are difficult to construct (8). Greater hydrothermal input to the oceans also accounts for the larger silica fluxes required to form the cherts, a flux that was attributed to increased volcanic input (46, 47) or diagenetic alteration of clays (48).

The Sr/Ca ratios from samples of well-preserved fossil planktonic foraminifera collected from throughout the Pacific basin show a significant decrease of 15 to 25 percent during the Eocene and the late Miocene (Fig. 1), a finding that has been attributed to an increased hydrothermal supply of Ca^{2+} during these periods (49). Most deep pelagic sediments are calcite, and so any increase in CaCO_3 deposition concordant with increased oceanic input of hydrothermal Ca^{2+} might be less evident than that of other components. Nevertheless, summaries of carbonate accumulation indicate a maximum during the Eocene (50, 51) when accumulation rates more than doubled (Fig. 1). A significant increase in hydrothermal activity also would be likely to change the pattern of carbonate deposition. Increased CO_2 concentrations in deep waters should lead to a shallower carbonate compensation depth (CCD) and lysocline, which would shift the concomitant increase in carbonate production toward shallower depositional environments. This is the pattern observed for the Eocene. The overall net increase in carbonate deposition during

this period is manifested as extensive shallow-water carbonate deposits (51), while deep-sea accumulation rates remained relatively low because of a pronounced global-scale shallowing of the CCD (52).

These observations strongly support our steady-state assumption that increased hydrothermal Ca^{2+} inputs must have been rapidly balanced by increased CaCO_3 production and concomitant CO_2 generation. On the other hand, we realize that an accelerated rate of hydrothermal Ca^{2+} input prior to a new steady state also must have been of limited duration because of various chemical constraints involving Ca^{2+} . For example, CaCO_3 production could have been limited by the HCO_3^- supply from land. However, using contemporary HCO_3^- input rates to impose this constraint would neglect the possibility of a positive feedback loop between atmospheric CO_2 concentrations and the HCO_3^- supply; that is, higher atmospheric CO_2 concentrations may have resulted in increased weathering rates and correspondingly higher rates of HCO_3^- input. Fortunately, the stratigraphic record does offer a definitive constraint. The upper limit of Ca^{2+} concentration in ancient oceans is constrained by the solubility product of gypsum and could never have been more than about three times present-day levels or gypsum would occur as a common component of nonevaporitic marine sediments (53). Thus for any given level of hydrothermal activity it is possible to estimate the time span during which increased Ca^{2+} inputs

could have accumulated in the ocean before precipitating as gypsum. On the basis of the five- to tenfold increase in hydrothermal activity suggested by recent findings (26–28, 31), we calculate that this situation could have prevailed for a maximum of no more than about 10^6 years.

Some of the data we have discussed are not applicable to all parts of the Eocene world and thus, strictly speaking, have only regional implications. The paleobotanical (36–38), CaCO_3 deposition (50, 51), CCD (52), oxygen isotope (40, 41), and silicon data (44, 45) are from widespread areas and so can be considered global. The interpretations of the eolian data as to continental aridity and wind strength are based on North Pacific cores only (42, 43). The iron and hydrothermal component data come from the North and South Pacific (26, 33–35). The dearth of iron-related and eolian data from other oceans reflects a lack of appropriate experiments rather than a demonstrated absence of that particular factor.

We postulate a series of global-scale phenomena that should be, within the duration of the causative event and the response times of each type of indicator, isochronous. The stratigraphies and time scales used to date these separate phenomena are not all the same. Deep-sea sediment studies commonly are based on foraminiferal or nannofossil stratigraphies, which correlate reasonably well (CaCO_3 , Ca^{2+} oxygen isotopes, some iron, some silicon data). North Pacific eolian and hydrothermal sediment studies are based on less well-defined ichthyolith stratigraphy. Paleobotanical studies are based on pollen stratigraphies. All time scales are now in the process of being tied into the globally applicable geomagnetic-reversal time scale, but that effort is incomplete. As of this writing, we can say that, within the limits of present stratigraphic accuracy, the documented phenomena are consistent with a single global-scale hydrothermal event, but we cannot state the exact timing of these phenomena.

The data indicate that a severalfold increase in sea-floor hydrothermal activity, occasioned by the early Eocene tectonic activity, caused a CO_2 -induced global greenhouse effect. The several other predicted results of increased hydrothermal activity also occurred: changes in global climate, reduction in the intensity of atmospheric circulation, and increased deposition of ferruginous, opaline, and calcareous sediments. Other periods, more distant from the present, of global readjustment of spreading centers have also occurred and should

show similar effects. The most obvious of these is the Late Cretaceous, Coniacian to Campanian, which was characterized by tectonic reorganizations, warm climates, abundant carbonate sediments, and deep-sea cherts.

ROBERT M. OWEN

DAVID K. REA

Department of Atmospheric and
Oceanic Science, University of
Michigan, Ann Arbor 48109

References and Notes

1. S. Arrhenius, *Philos. Mag.* **5**, 237 (1896).
2. T. C. Chamberlin, *J. Geol.* **6**, 609 (1898).
3. R. Revelle, *Sci. Am.* **247**, 35 (1982).
4. G. M. Woodwell *et al.*, *Science* **222**, 1081 (1983).
5. Report of the Carbon Dioxide Assessment Committee, (National Academy of Sciences, Washington, D.C., 1983).
6. R. A. Revelle and H. A. Suess, *Tellus* **9**, 18 (1957).
7. L. A. Frakes, *Climates Throughout Geologic Time* (Elsevier, New York, 1979).
8. J. P. Kennett, *Marine Geology* (Prentice-Hall, Englewood Cliffs, N.J., 1982).
9. T. J. Crowley, *Rev. Geophys. Space Phys.* **21**, 828 (1983).
10. J. D. Hays and W. C. Pitman, *Nature (London)* **246**, 18 (1973).
11. F. T. MacKenzie and J. P. Pigott, *J. Geol. Soc. (London)* **138**, 183 (1981).
12. R. A. Berner, A. C. Lasaga, R. M. Garrels, *Am. J. Sci.* **283**, 641 (1983).
13. B. H. Wilkinson, A. R. Carroll, R. M. Owen, *Geol. Soc. Am., Abstr. Programs* **15**, 718 (1983).
14. J. M. Edmond, K. L. Von Damm, R. E. McDuff, C. I. Measures, *Nature (London)* **297**, 187 (1981).
15. CYAMEX Scientific Team, *ibid.* **277**, 2523 (1979).
16. RISE Project Group, *Science* **207**, 1421 (1980).
17. J. M. Edmond *et al.*, *Earth Planet. Sci. Lett.* **46**, 1 (1979).
18. J. M. Edmond *et al.*, *ibid.*, p. 19.
19. J. L. Bischoff and F. W. Dickson, *ibid.* **15**, 385 (1975).
20. M. J. Mottl and H. D. Holland, *Geochim. Cosmochim. Acta* **42**, 1103 (1978).
21. J. I. Drever, *The Geochemistry of Natural Waters* (Prentice-Hall, Englewood Cliffs, N.J., 1982).
22. M. Maybeck, *Rev. Géol. Dyn. Géogr. Phys.* **21**, 215 (1979).
23. D. K. Rea and K. F. Scheidegger, *J. Volcanol. Geothermal. Res.* **5**, 135 (1979).
24. J. P. Kennett, A. R. McBirney, R. C. Thunell, *ibid.* **2**, 145 (1977).
25. W. C. Pitman III, *Geol. Soc. Am. Bull.* **89**, 1389 (1978).
26. M. Leinen and D. Stakes, *ibid. (Part I)*, **90**, 357 (1979).
27. Leg 92 Staff, *Nature (London)* **304**, 16 (1983).
28. Leg 92 Staff, *Geotimes* **28**, 16 (September 1983).
29. D. W. Handschumacher, *Am. Geophys. Union Monogr.* **19** (1976), p. 177; J. Mamerickx, E. Herron, L. Dorman, *Geol. Soc. Am. Bull.* **91**, 263 (1980).
30. D. K. Rea, *Geol. Soc. Am. Mem.* **154** (1981), p. 27.
31. J. Dymond, J. B. Corliss, G. R. Heath, *Geochim. Cosmochim. Acta* **41**, 741 (1977).
32. H. P. Johnson, personal communications.
33. D. S. Cronan, *Geol. Soc. Am. Bull.* **87**, 928 (1976).
34. T. L. Vallier, D. K. Rea, W. E. Dean, J. Thiede, C. G. Adelseck, *Init. Rep. Deep Sea Drill. Proj.* **62**, 1031 (1981).
35. M. Leinen and G. R. Heath, in preparation.
36. E. Dorf, *Problems in Palaeoclimatology*, A. E. M. Navin, Ed. (Interscience, London, 1964), pp. 13-30.
37. J. A. Wolfe, *Am. Sci.* **66**, 694 (1978).
38. R. N. L. B. Hubbard and M. C. Boulter, *Nature (London)* **301**, 147 (1983).
39. J. P. Kennett, *J. Geophys. Res.* **82**, 3843 (1977).
40. N. Shackleton and A. Boersma, *J. Geol. Soc. London* **138**, 153 (1981).
41. S. M. Savin, *Annu. Rev. Earth Planet. Sci.* **5**, 319 (1977).
42. T. R. Janacek and D. K. Rea, *Geol. Soc. Am. Bull.* **94**, 730 (1983).
43. T. R. Janacek, *Init. Rep. Deep Sea Drill. Proj.*, in press.
44. M. Leinen, *Geol. Soc. Am. Bull. (Part II)* **90**, 1310 (1979).
45. J. Thiede, J. E. Strand, T. Agedstein, *Soc. Econ. Paleontol. Mineral. Spec. Publ.* **32** (1981), p. 67.
46. S. E. Calvert, *Nature (London)* **234**, 133 (1971).
47. G. R. Heath and R. Moberly, *Init. Rep. Deep Sea Drill. Proj.* **7**, 991 (1971).
48. T. G. Gibson and K. M. Towe, *Science* **172**, 152 (1971).
49. D. W. Graham, M. L. Bender, D. F. Williams, L. D. Keigwin, Jr., *Geochim. Cosmochim. Acta* **46**, 1281 (1982).
50. T. R. Worsley and T. A. Davies, *J. Sediment. Petrol.* **49**, 1131 (1979).
51. T. A. Davies and T. R. Worsley, *Soc. Econ. Paleontol. Mineral. Spec. Publ.* **32** (1981), p. 169.
52. Tj. H. van Andel, J. Thiede, J. G. Sclater, W. W. Hay, *J. Geol.* **85**, 651 (1977).
53. H. D. Holland, *Geochim. Cosmochim. Acta* **36**, 637 (1972).
54. We thank our colleagues on the *Glomar Challenger* during DSDP Leg 92 for numerous discussions on the nature of sea-floor hydrothermal activity. We thank W. R. Kuhn, J. G. Walker, N. G. Pisias, and T. R. Janacek who reviewed the manuscript and provided helpful suggestions. This research was supported in part by a Rackham Faculty Research Award and by the National Science Foundation (grant OCE-8410034).

13 August 1984; accepted 1 November 1984

Plasmodium falciparum Malaria: Band 3 as a Possible Receptor During Invasion of Human Erythrocytes

Abstract. Human erythrocyte band 3, a major membrane-spanning protein, was purified and incorporated into liposomes. These liposomes, at nanomolar concentrations of protein, inhibited invasion of human erythrocytes in vitro by the malaria parasite *Plasmodium falciparum*. Liposomes containing human band 3 were ten times more effective in inhibiting invasion than those with pig band 3 and six times more effective than liposomes containing human erythrocyte glycophorin. Liposomes alone or liposomes containing erythrocyte glycolipids did not inhibit invasion. These results suggest that band 3 participates in the invasion process in a step involving a specific, high-affinity interaction between band 3 and some component of the parasite.

Malaria remains a major public health problem in many areas of the world, with an estimated 150 million cases resulting in 2 million deaths each year (1). Victims are inoculated by mosquito bite with the sporozoite stage of the malarial parasite, and the sporozoites rapidly invade hepatic parenchymal cells and differentiate into merozoites. The merozoites are released into the circulation, where they invade erythrocytes. Infected erythrocytes soon rupture, releasing multiple merozoites that invade other erythrocytes, leading to chronic parasitemia. Invasion of erythrocytes is a multistep process that involves (i) attachment of merozoites to the erythrocyte membrane in a random orientation; (ii) reorientation of the attached merozoites such that the apical end of the parasite is opposed to the erythrocyte membrane; (iii) formation of a junction between the apical end of the merozoite and the erythrocyte membrane; and (iv) invagination of the erythrocyte membrane around the attached merozoite to form a vacuole inside the erythrocyte (2).

Several lines of evidence indicate that the invasion process requires specific interactions between the merozoite and the host erythrocyte (3). Erythrocyte membrane proteins glycophorins A, B, and C have been implicated as one of the attachment sites for *Plasmodium falciparum* (3), the species that causes the most virulent form of human malaria. Invasion of erythrocytes by *P. falciparum* in vitro has been reduced by genetic

deficiency of glycophorins (4), digestion of glycophorin with trypsin or neuraminidase (5), and addition of isolated glycophorin to the assay medium (5). Friedman *et al.* (6) suggested that glycophorins A and B are involved in a relatively nonselective, charge-mediated attachment between merozoites and the red cell membrane, since various polyanions also inhibit invasion and since orosomucoid, a serum sialoglycoprotein unrelated to glycophorin, restores the invasion capacity of erythrocytes depleted of glycophorins (6).

Band 3, a major cell-surface protein in erythrocyte membrane, is a logical candidate to mediate specific red cell associations with malarial parasites. In support of this idea, Miller *et al.* (7) found that monoclonal antibody against rhesus monkey band 3 blocks invasion of rhesus erythrocytes by *Plasmodium knowlesi* parasites. We report here that human erythrocyte band 3 incorporated into liposomes is a potent inhibitor of invasion of human erythrocytes by *P. falciparum*, further supporting the hypothesis that band 3 participates in a high-affinity interaction with merozoite surface components.

Band 3 was purified from human erythrocyte ghosts by selective extraction of peripheral membrane proteins, followed by solubilization of membranes with nonionic detergent and fractionation of the detergent extract by ion-exchange chromatography (Fig. 1). Band 3 is not soluble in the absence of deter-